RELATION OF INITIAL SPECIMEN STATE AND PARTICLE PROPERTIES TO THE BREAKAGE POTENTIAL OF GRANULAR SOILS

Jason T. DeJong, Assistant Professor, University of Massachusetts Amherst
G. Geoffrey Christoph, Graduate Researcher, University of Massachusetts Amherst

ABSTRACT
The breakage potential of granular soils is of increased interest given recent observations of zones of crushed particles adjacent to piles, penetrometers (e.g. CPT), and other systems where load transfer primarily occurs through interfacial behaviour. A number of previous studies have focused on developing parameters to quantify crushing (e.g. Leslie 1975, Hardin 1985). However, the role of a number of factors on the magnitude of crushing has not been comprehensively examined. Therefore, the contribution and interaction of the initial specimen state, the particle properties, and the magnitude of stress is examined herein. For each soil a threshold stress level and void ratio were identified. This threshold condition reflects a transition from behaviour dependent on the initial specimen state to behaviour independent of the initial specimen state and corresponds to the initial intersection with the normal compression line. Finally, the effect of changes in specimen state on the hydraulic conductivity is examined preliminarily.

RÉSUMÉ
Le potentiel de rupture des sols granulaires est des plus grandes observations récentes données par intérêt des zones des particules écrasées à côté des piles, les pénétromètres (e.g. CPT), et d'autres systèmes où le transfert de charge se produit principalement par le comportement dièdre.Un certain nombre d'études précédentes se sont concentrées sur des paramètres se développants pour mesurer l'écrasement (e.g. Leslie 1975, Hardin 1985).Cependant, le rôle d'un certain nombre de facteurs sur l'importance d'écrasement n'a pas été largement examiné. Par conséquent, la contribution et l'interaction de l'état initial de spécimen, des propriétés de particules, et de l'importance de l'effort est examinée ci-dessus.Pour chaque sol un niveau d'effort de seuil et un rapport vide ont été identifiés.Cet état de seuil reflète une transition de personne à charge de comportement sur l'état initial de spécimen au indépendant de comportement de l'état initial de spécimen et correspond à l'intersection initiale à la ligne normale de compression.En conclusion, l'effet des changements de l'état de spécimen sur la conductivité hydraulique est examiné préalablement.

1. INTRODUCTION

Crushing occurs in single particle failure, one-dimensional compression, and through shear failures. The effects of particle crushing may include a decrease in volume, change in strength (presence of particles not carrying load), or generation of fines. These mechanisms have an impact on a wide variety of fields and disciplines, including geotechnical engineering, rock mechanics, oil production, and on the pharmaceutical industry. Terzaghi (Terzaghi et al. 1996) first reported the effects of particle crushing while extracting oil cores, noting a decrease in grain size and an increase in particle angularity.

Particle crushing has also been observed in a variety of geotechnical systems including piles, penetrometers, and filters. Zones of crushed particles have been observed adjacent to piles and penetrometers (White 2002) as well as within many systems where load transfer occurs primarily through interfacial behaviour (Westgate and DeJong 2004). Particle crushing may also cause a change in filter gradation below earth dams and lead to piping (Valdes 2002) and possible failure.

2. PREVIOUS RESEARCH

High pressure oedometer testing has been the conventional method used to study specimen crushing although high pressure conventional and true triaxial devices have be implemented as well. In the oedometer a vertical stress is applied axially while lateral expansion is restricted by a rigid boundary. A diameter of 50 mm with a sample height of 10 to 20 mm to alleviate sidewall friction for fine-grained sand is common (Nakata et al. 2001a, b). It is important to recognize that particles may fail due to shear as well as compression. By the Mohr circle for strain, in a 1-D oedometer test the shear strain is equal to one half the vertical strain.

Particle crushing has been shown to be dependent upon both initial specimen conditions and single particle properties. Stress level, void ratio, and initial grain size distribution are the primary specimen conditions that have been examined. The observed increase in crushing with an increase in global (applied) stress level is due to the global stress increasing the stress applied to each particle in the matrix (Hardin 1985). With discrete contacts existing at particle-particle contacts, the contract stress is orders of magnitude higher than the applied global stress. These high contact stresses often are the initiators of particle crushing. A decrease in void ratio, which is directly related to porosity and relative density, results in a decrease in the extent of breakage at a given stress level (Hardin 1985, Nakata et al 2001a, Vallejo 1995). Insight can be gained through the coordination number; as the void ratio decreases, the number of particle contacts (coordination number) increases, which results in a more stable structure that has greater resistance to crushing (Valdez 2002). The initial grain size distribution directly influences specimen crushability through the coordination

number as well. The coordination number for a well graded soil is higher than for a poorly graded soil, resulting in a more stable structure and lower particle-particle contact stresses for a given applied global stress (Hardin 1985, Nakata et al 2001a, Fukumoto 1992).

Single particle properties such as size, shape, mineralogy, and hardness also directly influence particle crushing (Hardin 1985, McDowell and Bolton 1998, and Lade et al. 1995). Increased crushing with an increase in particle size for a given global stress is due to the force (or contact stress) per particle increasing with particle size. This can be approximated by

$$F_{particle} = \sigma_{global} \times D_{50}^{2} \quad [1]$$

where $F_{particle}$ is the force per particle (divide by contact area to obtain contact stress), σ_{global} is the globally applied stress, and D_{50} is the average particle size by weight. Particle shape directly influences the modes of particle breakage also. Generally breakage of rounded particles occurs as local contact bearing failure or particle splitting, which results in a more pronounced compression yield stress. Angular particle crushing occurs through breakage of asperities and subsequently the generation of more fines. Material hardness, which can be quantified through either Mohs hardness scale or microhardness indentation tests, is directly correlated with the magnitude of applied stress at the onset of particle breakage. For example, crushing of calcareous sand is initiated at about 1/10 the applied stress required for crushing of silica sands. Finally, the mineral structure of the material, including fracture planes and the molecular structure, can result in preferential planes of failure and behaviour that deviates from isotropic material behaviour.

More recently a series of researchers (e.g. McDowell and Bolton 1998, Nakata et al. 2001b) have related single particle strength tests to specimen test behaviour. Single particles are compressed between two load platens at a constant rate of strain, a test conceptually similar to the Brazilian tensile test for rock. The maximum force applied prior to crushing is termed the crushing strength of the particle. The contact conditions (or coordination number) differ substantially in the single particle test as only two contacts exist (one against each platen) whereas particles will have multiple contacts within a specimen (Valdez 2002).

2.1 Breakage Criteria

Various methods and criteria have been proposed to quantify the extent of damage a specimen undergoes during loading. Specimen damage can be captured easily through quantifying changes in the grain size distribution (GSD). The attractive simplicity of sieve analysis has led to this being the predominant approach for assessment, although more complex microscopy methods are being introduced.

A selection of a number of previously proposed breakage criteria based on changes in GSD are summarized here (Figure 1). Breakage is determined by a difference between the pre- and post- test GSD curves, and may be quantified by differences with respect to the percent finer for a particle (sieve) size or the differences with respect to a certain percent finer (passing). Lee and Farhoomand (1967) compute the ratio of the D_{15} (15% finer by mass) pre- and post- GSD while Datta et al. (1979) compute the same ratio for D_{10} (10% finer by mass). Leslie proposes two criteria; difference in percent finer by mass on the sieve in which 100% of the initial soil was retained (1963) and on the sieve in which 90% of the initial soil was retained (Figure 1) (1975).

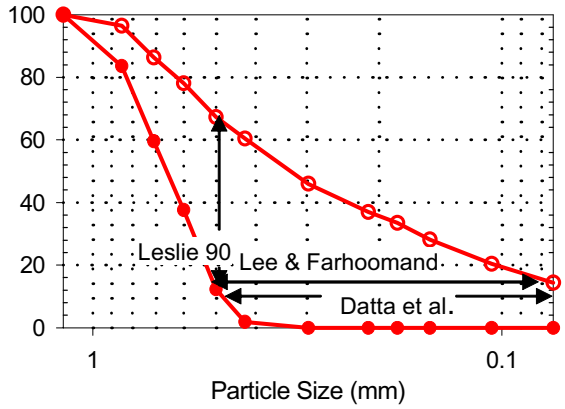

Figure 1. Select breakage criteria Based on Single Parameter Analysis.

An arguably more comprehensive method proposed by Hardin (1985) considers the entire grain size distribution curve for all particles sizes above 0.075 mm (#200 sieve). The breakage criteria, B_R, is defined as:

$$B_R = B_T/B_P \quad [2]$$

where breakage potential (B_P) is defined as the area above the initial pre-test grain size distribution curve, and total breakage (B_T) is defined as the area between the pre- and post- test grain size distribution curve. Since this criteria considers the entire GSD it may be more suitable for a wide range of materials.

3. MATERIALS AND METHODS

3.1 Granular Materials

Uniformly graded sands and glass beads were used in testing. Sands used include Ottawa 20-30, Q-rok, and Unimin. Particle shape was varied by the selection of two subangular sands (Unimin and Q-rok) and one subrounded sand (Ottawa), all with similar size and gradation. Glass beads were used as an extreme case of almost perfect spheres. Table 1 presents properties of the sands and glass beads along with single particle crushing strength determined using the method presented earlier (McDowell and Bolton 1998, Nakata et al. 2001a, b). As evident there was a general trend of a decrease in particle strength with an increase in particle aspect ratio.

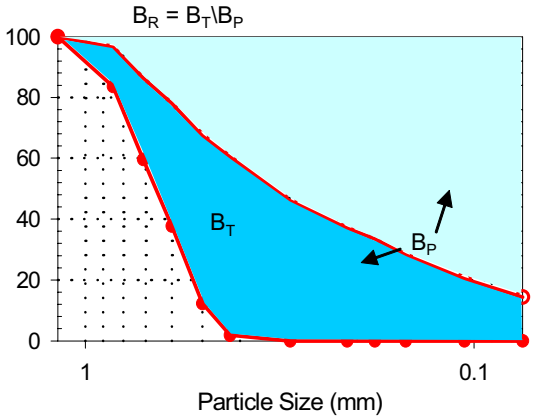

Figure 2. Schematic Representation of Hardin's Relative Breakage.

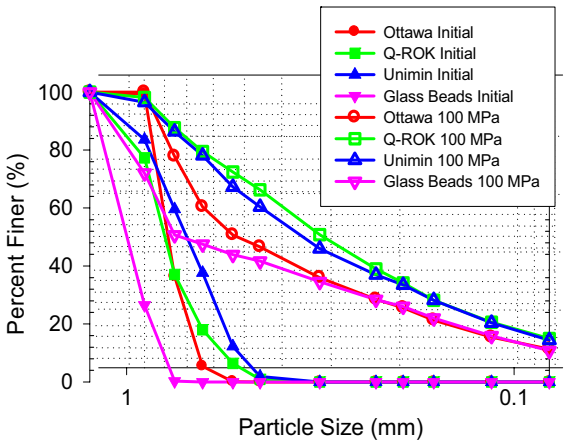

Figure 3. Grain Size Distribution for All Sands and Glass Beads.

The grain size distributions (GSD) for the sands and glass beads are presented in Figure 3. Curves of virgin material are presented with a companion post-test GSD curve from a specimen loaded to 100 MPa. Post-test curves for the sand are from specimens prepared at an initial relative density of 65% while for the glass beads the specimen was prepared to an initial relative density of 10%.

3.2 Test Apparatus

A high-pressure oedometer was used to perform testing (Figure 4). The vertical stress was applied manually through the use of a hydraulic piston, and readings of both load and displacement were taken using a 445 kN (100 kip) load cell and an LVDT through GeoTac data acquisition software.

Samples were prepared to a target relative density (D_R) through the use of a calibrated pluviator with an accuracy of +/- 3%. A sample diameter of 63.5 mm was used, slightly larger than that suggested by Nakata et al. (2001a), in order to accommodate the pluviation device. A sample depth of 20 mm was used to provide sufficient sample for subsequent sieve analysis. It is noted that specimens prepared with heights between 5 and 30 mm yielded the same GSD results in a parametric study, indicating minimal influence of wall friction and the repeatability of results. Sample height was controlled through the use of a calibrated vacuum that removed excess particles and provided a level surface for seating of the oedometer top cap. A measurement of sample height was taken after seating to verify the initial relative density.

3.3 Test Program

Specimens 63.5 mm in diameter and 20 mm in height were prepared at relative densities of 35%, 50%, 65%, 80%, and 95%. Glass beads were prepared to the same dimension, but with relative densities of 10% and 100% due to the extremely low angle of repose (<5°) and a small range between e_{min} and e_{max} (Table 1). Tests were conducted to stress levels of 10, 20, 40, 70, 80 and/or 100 MPa using a hydraulic pump. In total, more than 100 tests were performed. Grain size distribution characteristics were determined pre- and post- testing and used to evaluate breakage criteria.

Table 1. Summary of Sand and Glass Beads Properties.

Sand	D_{50} (mm)	C_u [1]	C_c [2]	G_s [3]	e_{max} [4]	e_{min} [5]	Roundness [6]	Aspect Ratio [7]	Fracture Strength [8] (MPa)
Ottawa 20-30	0.74	1.06	0.98	2.64	0.74	0.51	0.43	1.22	12.8
Unimin	0.66	1.48	0.62	2.63	1.06	0.73	0.44	1.45	8.1
Q-ROK	0.75	1.47	1.09	2.64	1.14	0.80	0.48	1.34	4.8
Glass Beads	0.95	1.25	1.13	2.50	0.73	0.58	0.39	1.00	21.6

[1] $C_u = D_{60}/D_{10}$ (ASTM D2487-93), [2] $C_c = D_{30}^2/(D_{10} * D_{60})$ (ASTM D2487-93), [3] AASHTO T133, [4] ASTM D4254-91, Method B, [5] ASTM D4253-93, Method 2A, [6] Roundness = Perimeter/4*π*Area, [7] Aspect Ratio = Major axis/Minor axis, [8] Fracture Strength = Force at failure/diameter². (McDowell and Bolton 1998)

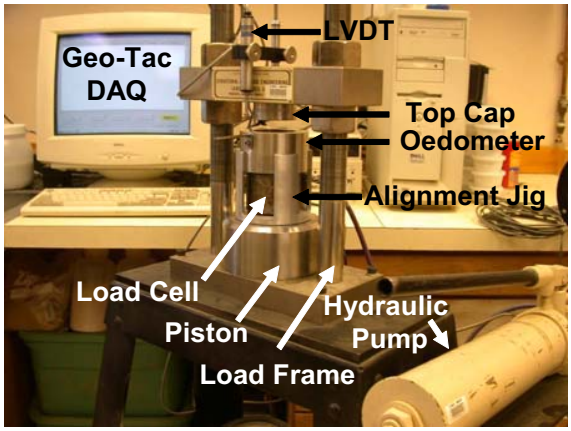

Figure 4. Photograph of High Pressure 1-D Oedometer.

4. RESULTS AND DISCUSSION

4.1 Effect of Particle Properties and Stress Level

The loading path of crushing tests performed to a maximum stress of 100 MPa as well as data points indicating the final state for tests completed at lower stress magnitudes (5 MPa to 100 MPa) are shown in Figure 5. All sand samples prepared for this phase of testing were pluviated to an initial relative density of 65%, while glass beads were prepared at an initial relative density of 10%. Since all sand tests were performed at the same initial relative density and over the same range of stresses, any differences in behaviour are due to variations in specimen and single particle properties. These include particle shape, size, and hardness.

As evident in Figure 5, subangular particles (i.e. Unimin and Q-rok) exhibit greater initial strain and a greater overall strain that subrounded Ottawa sand. Inelastic strain occurs at low stresses due to asperity breakage of angular particles. Subangular sands Unimin and Q-rok reach volumetric strains in excess of 30%. Recalling Mohr circle for strain for 1-D compression, shear strains exceed 15%.

Verification of particle shape dependency comes from the stress strain behaviour of glass beads. There is a distinct point where elastic compression ends and particle breakage begins. Once the initial stress chains are broken within the conjoined structure of the beads, through the failure of one or several particles, there is a rapid straining of the sample at an almost constant stress (about 30 MPa). The rapid straining is a product of a decrease in coordination number on particles touching those that have broken. Stress chains reorient themselves and become higher intensity in certain areas that now have particles present not carrying load. Therefore, without an increase in overall sample stress, individual particle stresses will increase and cause particle failure and sample straining. Once failure of the particles has occurred, about 40 MPa for the glass beads, the coordination number has again increased and a new sample structure is realized allowing the rounded beads to exhibit the same stress strain behaviour as subangular sand.

Glass beads exhibit one extreme of 1-D compression behaviour. Subrounded Ottawa sand shows little initial strain and a distinct transition into inelastic behaviour with particle breakage, similar to the behaviour of glass beads. However, overall strain in the Ottawa sand is much less than that of subangular sand, and the glass beads that exhibit the same stress strain behaviour as the subangular sand after particle breakage has occurred. It is hypothesized that for Ottawa sand asperity breakage is sufficiently reduced while at the same time particle shape is irregular enough that coordination number will vary from particle to particle. Ottawa sand does not undergo the

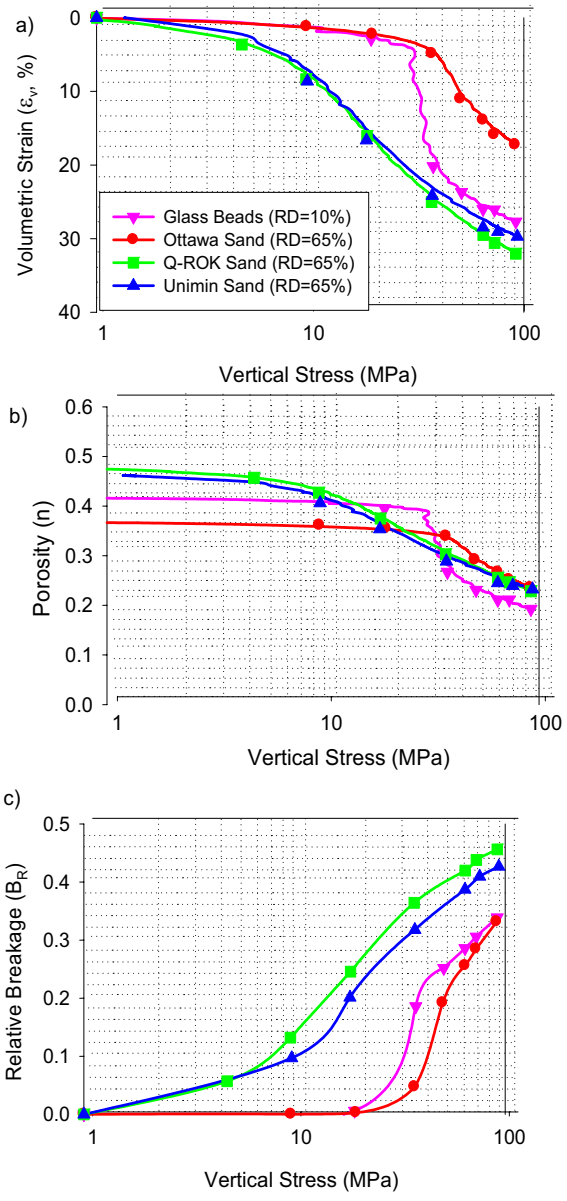

Figure 5. Strain, Porosity, and Relative Breakage Versus Variation in Stress Level.

intense localization of stress chains that occurs within the perfectly round beads. Subrounded Ottawa specimens have an initial structure similar to that of the glass beads, but particle breakage must occur in a mode that allows less drastic changes in coordination number and a bridging effect of the stress chains.

Changes in porosity of the samples were greatest for subangular sands, displaying a decrease of almost 50%. Porosity changes with increasing stress was similar to the strain behaviour for each sand and glass beads. This is predicted through the following equations:

$$\varepsilon_v = (e-e_0)/(1+e_0) \quad [3]$$

$$e = n/(1-n) \quad [4]$$

where ε_v is the vertical strain, e_0 is the initial pre-test void ratio, e is the void ratio at a given stress level, and n is the porosity at a given stress level.

Interestingly, regardless of particle shape, all silica sands approach a similar porosity at 100 MPa (n = 0.23), and glass beads had an ultimate porosity that was lower (n = 0.19). The trend lines plotted for the round particles (Ottawa, glass beads) in Figure 6 a) and b) overshoot the trend lines of the angular particles (Q-rok, Unimin) because of a stronger structure and the lack of asperity breakage at lower stresses.

Using Hardin's (1985) relative breakage criteria, the extent of breakage was quantified at selected stress levels (all data points shown in Figures 6a). As presented previously, the actual change in the grain size distributions for sands and glass beads tested to 100 MPa and prepared at initial relative densities of 65% and 10% for the sands and glass beads, respectively, are shown in Figure 3.

Both the trend of relative breakage with stress level and the total magnitude of breakage at 100 MPa (B_R = 0.34 for glass beads, 0.33 for Ottawa, 0.43 for Unimin, and 0.46 for Q-rok) are similar for particles of similar shape. As expected, subangular particles that fail primarily through breakage of asperities generate considerable fines. The trend shown in Figure 5c verifies that fines are generated at stresses as low as 1 MPa for subangular samples in 1-D compression. At 100 MPa the trend remains the same between Q-rok and Unimin, and the relative breakage remains higher than that of rounded and subrounded particles.

Glass beads and Ottawa sand exhibit similar breakage behaviour to one another. Up to about 20 MPa there is negligible fines generation because failure of the particle occurs by splitting at higher stress and not by asperity breakage. Similar to the behaviour shown on the stress strain plot, once inelastic strain is initiated there is a rapid increase in the relative breakage. After the onset of particle breakage the trend in breakage is similar for all samples regardless of shape.

4.2 Effect of Relative Density

The influence of relative density was examined for the sands and glass beads by testing specimens prepared over a wide range of initial relative densities. Figure 6 contains plots of volumetric strain, porosity, and Hardin's breakage criteria versus applied vertical stress for all sands and glass beads. All sand samples prepared for this phase of testing were pluviated to an initial relative density between 35% to 95%, while glass beads were prepared to relative densities of 10% and 100%.

All samples exhibit behaviour whose characteristics show some degree of dependence on the initial relative density. Ottawa sand and glass beads display a distinct transition from elastic to inelastic compression while Unimin and Q-rok display inelastic breakage at low stresses and as a result do not exhibit such a distinct transition.

A threshold stress value where the porosity becomes independent of initial density is evident in Figures 6 a) and b). Clearly displayed by the angular soils, behaviour of all specimens irrespective of the initial relative density converges once the threshold stress value has been reached. The threshold stress value for Unimin and Q-rok is about 20 MPa. For the rounded soils (Ottawa, glass beads) the threshold stress value is less distinct although convergence is observed at a stress level of about 60 MPa. Above the threshold stress, stress-strain behaviour is the same within each sample type and is offset only by the initial relative density effects up to the threshold stress.

The threshold stress value, as well as an "overshoot" phenomenon (trend lines for specimens with a higher relative density cross the trend lines for specimens with a lower relative density) for rounded particles, is better defined in the porosity-stress behaviour (Figure 6b). Shown clearly for the Ottawa sand, there is a link between the overshoot and the stress-strain behaviour. The point at which there is a transition in the porosity-strain behaviour corresponds to the transition at which specimens with lower relative densities diverge from the trend in stress-strain behaviour and become inelastic due to the onset of particle breakage.

Samples with a higher initial relative density have a lower porosity and therefore a denser packing of particles. A denser packing corresponds to a higher coordination number. Although overall stress on a sample may be the same, the denser sample with a higher coordination number has a lower particle-particle contact stress. Therefore elastic behaviour is prolonged to higher global stress levels.

Angular particles do not undergo this phenomenon because particles fail in a different manner. Round particles in a packing exhibit a strong overall structure, while angular particles easily break asperities and constantly redistribute stress chains.

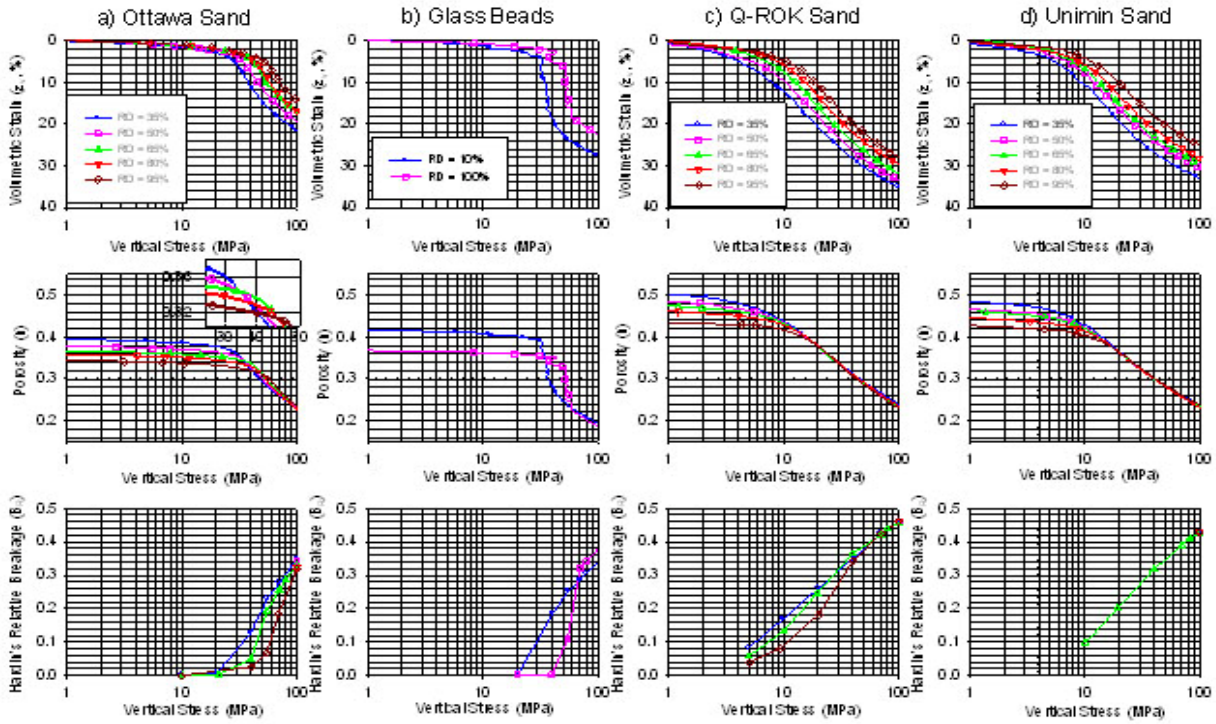

Figure 6. Strain, Porosity, and Relative Breakage Versus Stess Level for a Range of Relative Densities.

5. IMPLICATIONS ON HYDRAULIC CONDUCTIVITY

Effects of sample straining, changes in porosity, and breakage quantification with respect to grain size have been examined, but have not been extended to quantify the influence on hydraulic conductivity. Herein the effect of crushing on hydraulic conductivity is investigated through computing pre- to post- test ratios based on empirical equations. Experimental research is currently underway to validate these ratios.

Empirically estimated ratios of the coefficient of hydraulic conductivity (k) from pre- to post- testing at 65% initial relative density at 100 MPa for all sands is presented in Table 2. Testing for the loose glass beads was at 10% initial relative density and 100 MPa, while the dense glass beads were at 100% initial relative density and 100 MPa.

Taylor (1948) proposed a relationship between the hydraulic conductivity and void ratio (e):

$$k_1 : k_2 = (C_1 e_1^3)/(1+e_1) : (C_2 e_2^3)/(1+e_2) \quad [5]$$

where C_1 and C_2 are coefficients that depend on soil structure and are approximately equal for clean sands with less than 5% less than 0.075 mm (#200 sieve) (Holtz and Kovacs 1981). Coefficients C_1 and C_2 depend on soil structure, which is known to change once particle crushing occurs. In addition, more than 5% of the GSD is less than 0.075 mm above stress levels of approximately 65, 50, 40,

and 40 MPa for Ottawa sand, glass beads, Q-rok sand, and Unimin sand, respectively. Therefore, an assumption that the coefficients are equal is not fully valid for the analysis of crushing on hydraulic conductivity.

Kozeny-Carmen (modified from Bear 1972) proposed a relationship for hydraulic conductivity (K) based on porosity and effective grain size D_{50} (size at which 50% is finer by mass) for granular materials. Since both the porosity and D_{50} changes with crushing and these changes were quantified through the testing program this equation is conceptually more appropriate for prediction of changes in the hydraulic conductivity due to crushing. The hydraulic conductivity can be computed as follows:

$$K = (\rho_w g/\mu)\ (n^3/(1-n)^2)\ ((D_{50})^2/180) \quad [6]$$

where ρ_w is the density of water, g is the gravitational constant, μ is the viscosity of water, and n is porosity. As presented in Table 2, initial hydraulic conductivity values predicted by this equation range from 3.65×10^{-4} to 1.03×10^{-3} cm/s, which are reasonable values for cleans sands.

If one assumes ρ_w, g, and μ to be constant, a ratio may be developed to determine the magnitude of change in k without knowledge of the initial hydraulic conductivity as follows:

$$K_1:K_2=(n_1^3/(1-n_1)^2)\ ((D_{50})_1^2/180) : (n_2^3/(1-n_2)^2)\ ((D_{50})_2^2/180) \quad [7]$$

Table 2. Summary of Permeability Relationships.

	Properties @ 0 MPa			Properties @ 100 MPa			Taylor[1]	K-C[2]	
Sand	D_{50} (mm)	e	n	D_{50} (mm)	e	n	$k_1 : k_2$	K_1 (cm/sec)	$K_1 : K_2$
Ottawa 20-30	0.74	0.580	0.367	0.49	0.308	0.235	5.53	$3.65*10^{-4}$	7.06
Unimin	0.75	0.915	0.478	0.29	0.301	0.231	19.08	$1.22*10^{-3}$	40.90
Q-Rok	0.66	0.847	0.459	0.33	0.298	0.230	16.14	$7.77*10^{-4}$	22.65
Glass Beads (D_R=10%)	0.95	0.713	0.416	0.51	0.238	0.192	19.43	$1.03*10^{-3}$	24.96
Glass Beads (D_R=100%)	0.95	0.583	0.368	0.70	0.228	0.186	12.97	$6.08*10^{-4}$	10.79

[1]Taylor (1948) = ratio of coefficient of permeability (k)
[2]Kozeny-Carmen (modified from Bear 1972) = ratio of hydraulic conductivity (K)

Table 2 presents ratios of the hydraulic conductivity using Equation 7. As evident, decreases in permeability range from about 7 for Ottawa 20-30 sand to more than 40 for Unimin sand.

6. CONCLUSIONS

An experimental program has been performed to evaluate the effect of specimen and particle properties on the crushing behaviour of granular soils and examine possible associated changes in the hydraulic conductivity. The following observations have been made:

-
- Particle angularity results in asperity mode breakage, resulting in a transition to inelastic behaviour at relatively low global stresses.
-
- Spherical and sub-rounded materials have a stable initial structure that results in pronounced yield at stresses higher than angular particles. An "overshoot" behaviour dependent on the initial density (coordination number) was also observed.
- Hardin's breakage criteria was shown to successfully capture breakage evolution with stress level.
- Empirical estimates of changes in hydraulic conductivity indicate up to two orders of magnitude decrease due to particle crushing.

The research results presented herein are a subset of an ongoing investigation to assess changes in soil properties with crushing induced by both compression and shear loading modes. In its entirety the objective of this investigation is to assess the relative importance of crushing on the performance of interface dependent geotechnical systems.

7. REFERENCES

Bear, J. 1972. *Dynamics of Fluids in Porous Media*, United States, Elsevier, New York.

Fukumoto, T. 1992. Particle breakage characteristics of granular soils. *Soils and Foundations*, Vol. 32, pp. 26-40.

Hardin, B.O. 1985. Crushing of soil particles, *ASCE Journal of Geotechnical Engineering*, Vol. 111, pp. 1177-1192.

Holtz, R.D. and Kovacs, W.D. 1981. *An Introduction to Geotechnical Engineering*, United States, Prentice-Hall, New Jersey.

Lade, P.V., Yamamuro, J.A. and Bopp, P.A. 1996. Significance of particle crushing in granular materials, *ASCE Journal of Geotechnical Engineering*, Vol. 122, pp. 309-316.

Lee, K.L. and Farhoomand, I. 1967. Compressibility and crushing of granular soil. *Canadian Geotechnical Journal*, Vol. 4, pp. 68-86.

Leslie, D.D. 1963. Large scale triaxial tests on gravely soils. *Proc. Of the 2nd Panamerican Conference on Soil Mechanics and Foundation Engineering*, Brazil, Vol. 1, pp. 181-200.

Leslie, D.D. 1975. Shear strength of rockfill. *Physical Properties Engineering Study No. 526*, US Army Corps of Engineers, p. 124.

McDowell, G.R. and Bolton, M.D. 1998. On the micromechanics of crushable aggregates. *Geotechnique*, Vol. 48, pp. 667-679.

Nakata, Y., Hyodo, M. Hyde, A., Kato, Y. and Murata, H. 2001. Microscopic particle crushing of sand subjected to high pressure one-dimensional compression, *Soils and Foundations*, Vol. 41, pp. 69-82.

Nakata, Y., Kato, Y., Hyodo, M. Hyde, A. and Murata, H. 2001. One-dimensional compression behaviour of uniformly graded sand related to single particle crushing strength, *Soils and Foundations*, Vol. 41, pp. 39-51.

Terzaghi, K., Peck, R.B. and Mesri, G. 1996. *Soil Mechanics in Engineering Practice*, 3'rd ed., United States, John Wiley, New York.

Valdes, J.R. 2002. *Fines migration and formation damage – microscale studies*, Georgia Institute of Technology Doctoral Thesis, United States.

Vallejo, L.E. 1995. Fractal analysis of granular materials, *Geotechnique*, Vol. 45, pp. 159-163.

DeJong, J.T. and Westgate, Z. (2004) "Role of particle crushing at the soil-structure interface during cyclic loading", *ASCE EM2004 Conference*, 5 p.

White, D.J. 2002. *An investigation into the behaviour of pressed-in piles*, University of Cambridge Doctoral Thesis, England.